General Disclaimer

One or more of the Following Statements may affect this Document

- This document has been reproduced from the best copy furnished by the organizational source. It is being released in the interest of making available as much information as possible.

- This document may contain data, which exceeds the sheet parameters. It was furnished in this condition by the organizational source and is the best copy available.

- This document may contain tone-on-tone or color graphs, charts and/or pictures, which have been reproduced in black and white.

- This document is paginated as submitted by the original source.

- Portions of this document are not fully legible due to the historical nature of some of the material. However, it is the best reproduction available from the original submission.

NASA TECHNICAL MEMORANDUM

NASA TM X-73677

NASA TM X-73677

EVALUATION OF INITIAL COLLECTOR FIELD PERFORMANCE AT THE LANGLEY SOLAR BUILDING TEST FACILITY

by Robert J. Boyle, Richard H. Knoll, and Ronald H. Jensen
Lewis Research Center
Cleveland, Ohio 44135

TECHNICAL PAPER to be presented at the
Tenth Annual Meeting of the American Section
of the International Solar Energy Society
Orlando, Florida, June 6-10, 1977

EVALUATION OF INITIAL COLLECTOR FIELD PERFORMANCE AT THE LANGLEY SOLAR BUILDING TEST FACILITY

Robert J. Boyle, Richard H. Knoll
National Aeronautics and Space Administration
Lewis Research Center
Cleveland, Ohio 44135

Ronald N. Jensen
National Aeronautics and Space Administration
Langley Research Center
Hampton, Va. 23665

ABSTRACT

The thermal performance of the solar collector field for the NASA Langley Solar Building Test Facility is given for October 1976 through January 1977. An 1180 square meter solar collector field with seven collector designs helped to provide hot water for the building heating system and absorption air conditioner. The collectors were arranged in 12 rows with nominally 51 collectors per row. Heat transfer rates for each row are calculated and recorded along with sensor, insolation, and weather data every 5 minutes using a mini-computer. The agreement between the experimental and predicted collector efficiencies was generally within five percentage points.

INTRODUCTION

The Energy Research and Development Administration and the National Aeronautics and Space Administration are jointly involved in several projects investigating the use of solar energy for heating and cooling of buildings. One such project is the Solar Building Test Facility (SBTF) located at the Langley Research Center in Hampton, Virginia (ref. 1). The SBTF consists of a 4645-square-meter (50 000-ft^2) single story office building that has been modified to accept solar heated water to help operate the building's absorption air conditioner and heating system. A 12-row 1180-square-meter (12 700-ft^2) solar collector field, currently utilizing seven different collector designs, provides the heated water, and a 114-cubic-meter (30 000-gal) tank is used for hot water storage. The SBTF was designed as an experimental test facility to provide: (1) comparative performance data on high performing collectors; (2) component and system performance of solar heating and cooling systems and interactions of the various elements, and (3) data on the durability, maintenance, and reliability of components. In addition, the solar system was designed to satisfy a major portion of the building's heating and cooling requirements.

The facility came on-line during mid-1976. The initial thrust of the research effort has concentrated on the performance of the seven different collector designs contained in the field. Work reported in reference 2 determined the baseline ("as received") performance of individual samples of the seven collector designs in a well controlled indoor solar test facility at the NASA Lewis Research Center. The indoor facility is described in reference 3. This paper presents the measured outdoor performance of the entire solar collector field for the period of October 1976 through mid-January 1977.

A brief description of the SBTF and its data handling and instrumentation system is included along with a description of the collectors used. Experimental performance comparisons of the seven collector designs are presented along with comparisons between measured performance and predicted performance based on the "as received" test data of reference 2. Finally, the effect of collector inlet temperature on collector efficiency is examined as well as the effect variations in the collector outlet temperature caused by expected flow variations within the collector rows.

EXPERIMENTAL APPARATUS

Facility description. - The Solar Building Test Facility (fig. 1) consists of a 4645-square-meter (50 000-ft^2) single story office building that has been modified to accept solar heated water to help operate its 2150 MJ/hr (170 ton) lithium bromide absorption air conditioner and its hot water heating system. The solar collector field adjacent to the building currently contains 1180 square meters (12 700 ft^2) of collectors and provides hot water for direct use in the building or for storage in a 114-cubic-meter (30 000-gal) tank. An additional storage tank is also available for later use for either hot water storage or chilled water storage if deemed desirable. Figure 2 gives a flow schematic for the SBTF. Further detail of the facility is given in reference 1.

Solar collector field. - The solar field (see fig. 1) is located on a plot of land adjacent to the office building and at ground level, rather than on the building roof; this location was selected to facilitate access to the experimental field for changing and/or servicing collectors. The collectors face due south and are tilted at 32° to the local horizontal. This particular tilt angle was selected to provide for the relatively high summer air conditioning requirements.

The collector field contains 12 collector rows connected in parallel between two 10.2 cm

(4.03 in.) main headers. There are nominally 51 collectors per row also connected in parallel as shown in figure 3. The row inlet and outlet headers are 4.09 cm (1.61 in.) in diameter. Steel braid reinforced rubber hoses run between the headers and the individual collectors. Bypasses are provided around the temperature control valves to insure that a minimum flow will always be maintained through the collectors. Each row can be valved out of the system if necessary. Air vents and relief valves are also included in all rows. Sufficient instrumentation is contained in each row to determine the net heat collected or lost on a continuous basis.

The initial mix of collectors for the SBTF and their location within the field is shown in figure 4. There are seven collector designs distributed among the 12 collector rows. Some collector designs are contained in more than one row; that is, rows 1, 2, and 7 are one design, rows 8 and 9 are a second design, and rows 10, 11, and 12 are a third design. Figure 5 is a photograph showing most of the collector designs contained in the field. Further detail on the various collector designs is given in Table I.

Instrumentation and data handling. - Instrumentation for the Solar Building Test Facility can be grouped into three general categories: (1) weather and insolation instrumentation, (2) collector field instrumentation, and (3) system instrumentation. In the first category data are taken on wind speed and direction, ambient temperature, humidity, and total and diffuse insolation in the horizontal plane. Insolation data are provided by two Eppley precision spectral pyranameters (model PSP). One unit incorporated a shadow band for determination of the diffuse insolation. Stated accuracy of the pyranameters was ±13.9 W/m^2 (±4.4 $Btu/hr\text{-}ft^2$).

Collector instrumentation is arranged to determine the performance of each row in the field as shown in figure 3. Temperature measurements are made on the row inlet and outlet headers with platinum resistance temperature sensors having an accuracy of ±0.2 C (±0.35° F). Accuracy of the center collector outlet temperature is ±0.8 C (±1.5° F) because of the larger temperature range covered. The flow rate for each row was measured by a turbine flowmeter with an expected accuracy of ±0.1 liter/sec (±0.15 gpm). The pressure drop across each row is monitored and recorded in order to spot long term changes due to fouling of the flow passages. No pressure drop data is reported herein.

Details of the temperature, pressure, and flow instrumentation for the complete solar system can be found in reference 1.

The data handling system utilizes a Xerox 514 minicomput both for processing the data and for providing future computerized control of various system functions. On-line data processing includes converting the raw data to engineering units as well as performing calculations to monitor the collector performance, solar system performance, and to account for energy usage or storage throughout the system. Presently 176 channels of data along with heat transfer calculations are recorded on magnetic tape for subsequent use. Data are taken continuously for alarm purposes, and are recorded at 5-minute intervals. Each recorded or displayed data point is averaged over a 10-second time interval.

The data handling system also includes a cathode ray tube (CRT) for data display and a line printer for hard copies of the CRT images. CRT images of all recorded data are available as well as images displaying calculated values of instantaneous, hourly and daily performance of the various collectors and the system (efficiency, heat transfer rates, energy used or stored, and the building energy requirements). Hard copies of daily performance summaries are available on demand.

RESULTS AND DISCUSSION

Experimental data taken on collectors. - Experimental data were taken for the period of October 1976 through mid-January 1977. Data automatically taken on each solar collector row are depicted by the results given in figure 6 for row number 10. The row flow rate, inlet and outlet temperatures, along with experimental efficiency are given for a typical day. Data were recorded every 5 minutes during daytime hours and every hour during nighttime hours. It can be seen that the experimental efficiency changes rapidly with changes in flow or temperature. This is due primarily to the thermal capacitance of the collectors. For example, it can be seen from figure 6 that after 11:00 there was a sharp decrease in the inlet temperature, but for almost an hour the outlet temperature decreased slowly. Consequently, during this time the efficiency increased sharply.

Also shown in figure 6 are the experimental and predicted efficiencies for the entire day from sunrise to sunset. The experimental efficiency is found from the heat gained by the fluid during the daytime and the total insolation. The predicted daytime efficiency is based on the analytic method described in appendix A assuming no thermal capacitance. It is apparent that, even when the thermal capacitance is neglected, there is reasonably good agreement between the predicted efficiency of 25 percent and the experimental efficiency of 28 percent for the day as a whole. The data typified by figure 6 are taken each day for each collector row.

Typical results for the entire solar collector field are shown in figure 7. This figure shows the efficiency for a whole day for each collector row on one of three different days. The collector efficiency shown is the daytime experimental efficiency. To obtain this efficiency the net amount of heat absorbed by the water during all of the daylight hours is divided by the total insolation incident on the collectors over the same time period. It would have been desirable to show data for all 12 collector rows for a single day. However, during this initial operational period, difficulty was experienced with some of the flowmeters, and some of the collectors had leakage or

local freeze up problems.

For nine of the 12 rows the data shown are for the same day. The collectors in rows 1, 2, and 7 are of the same type (two glass - selective paint), and the data show row 1 to have a significantly higher efficiency. This row had the most exposure to the reflecting gravel bed around the field (see fig. 1). A single spot check with a pyranameter taking measurements in the plane of the collectors between rows 1 and 2 verified the higher fluxes for the first row. No account was taken in the analysis of increased reflections due to the gravel bed. This could result in the experimental efficiency for the first row being slightly inflated. Rows 8 and 9 had collectors of the same type (single glass - black chrome) and show a significant difference in efficiency. On the average the difference in experimental efficiencies between rows 8 and 9 was about two percentage points. Rows 10, 11, and 12 contain two glass - black chrome collectors and show fair agreement. Row 3 contains the single glass - black nickel collectors and is also for the same day.

From data such as these, performance comparisons can be made on collectors of different designs under identical conditions of the same insolation, weather and field inlet temperature. The nature of the SBTF is such that these kinds of comparisons can automatically be made on a day to day basis for extended periods of time over a wide range of conditions.

Daily comparisons of experimental and predicted collector efficiency. - Data presented in Table II compare the measured experimental efficiencies with predicted efficiencies, for selected days throughout the test period. The days selected were those in which at least one row collected 210 MJ (0.2 MBtu) during the day. The dash notation throughout the table are days when the collector row was either shut down or the flowmetes were inoperative.

The predicted efficiency for each collector row was determined using the measured efficiency obtained from the NASA Lewis indoor solar collector test facility (ref. 2) and modifying this efficiency to account for conditions encountered in the outdoor tests at the SBTF. The results of the indoor tests yielded an empirical efficiency equation for each collector tested. The indoor test results were determined with the incident flux normal to the collectors and having no diffuse component. The ambient temperature was approximately 27 C (80° F) and the effective wind speed was 11 kph (7 mph) for these tests. Tests were conducted at flow rates of 24.4 kg/hr-m^2 (5 lb/hr-ft^2) and 48.8 kg/hr-m^2 (10 lb/hr-ft^2). The efficiency determined on the basis of the indoor test results was modified to account for the differences between the indoor test conditions and the conditions which prevailed during the SBTF testing. The modifications to the collector efficiency accounted for: (1) a decrease in the heat absorbed due to off normal incidence angles; (2) the difference in the flow rates; (3) difference in the wind speeds; and (4) an arbitrary decrease in transmittance due to dust on the outer cover. This efficiency calculation was made using the average values of the inlet and ambient temperatures, flow rate, wind speed, and insolation for the entire day. Appendix A gives further details of the analysis.

It can be seen from Table II that even though there is considerable variation between the predicted and experimental efficiencies on a daily basis, there is reasonably good agreement based on the average for the days of each month. The analysis uses the average conditions for the day, and these conditions vary due to both weather changes and the building's demand. Therefore, it is expected that the agreement should be better on a monthly basis than on a daily basis. It can be seen from the experimental data that the efficiency is generally greater for collectors with low emittance absorber plates. All of the collector designs had absorptance values approaching one. For collectors of identical construction the lower emittance of the black chrome collectors in rows 10, 11, and 12 resulted in significantly higher efficiencies than the higher emittance of the selective paint collectors in rows 1, 2, and 7. The collectors with the higher emittance coatings had the lower measured efficiencies. One interesting point is that the single glass - black chrome collectors (rows 8 and 9) performed nearly as well as the two glass - black chrome collectors (rows 10, 11, and 12). This was influenced to some degree by the low wind speeds measured at the SBTF site.

Overall the consistency in experimental data between rows with the same collector design was good. The agreement between the predicted and experimental efficiencies was reasonably good except for the one glass - black chrome collectors (rows 8 and 9). A general trend noted from Table II was that the predicted efficiencies tended to exceed the experimental efficiencies as time progressed. At this point the authors are not sure why this occurred.

Factors influencing the predicted efficiency. - Part of the difference between the predicted and experimental efficiencies could also be due to neglecting thermal capacitance effects. On almost every day the collector temperatures were higher at sunset than at sunrise. Consequently, some heat which was absorbed remained within the collectors and did not get included in the calculations. The thermal capacitance of the collectors is not known precisely, however, an estimate of the capacitive effects based on the temperatures at the beginning and end of each day show that the capacitive effects account for about 1.5 percentage points in the efficiency difference for December.

In addition to the capacitance effects it appears that flow variations through collectors within the row could contribute to the difference between the predicted and experimental efficiencies. The analysis reported in reference 4 gave the expected velocity distribution for the collectors within a row. The collector at the center of the row has the lowest velocity. The lower flow through the center collectors is caused by the use of constant diameter headers of finite size. If larger, but more expensive, headers were used, the variation in flow between collectors in a given row would be

less. For turbulent flow, such as was expected for most of the designs in the field, the velocity through the collector in the center of the row is expected to be 0.5 of the average velocity of the row over a wide range of flow rates. The velocity through the center collector was not measured, however, the outlet temperature for the center collector was measured. For a velocity ratio of 0.5 the temperature rise through the center collector would be twice the average rise for the row if the efficiency was not a function of flow rate. However, the efficiency is a function of the flow rate through the collector. Figure 8 gives the temperature ratio for the center collector as a function of row flow rate. There is reasonably good agreement between the experimental temperature ratio and predicted temperature ratio especially considering that the temperature difference in the denominator is only 10 C (18° F) at the highest experimental flow rate. It can be seen from the work in reference 5 that the effect of flow rate on collector efficiency is an asymptotic function. Therefore, the decrease in velocity through the collectors near the center of the row is not compensated for by the increase in velocity through the collectors near the ends of the row. There is a net loss in efficiency for the row as a whole. For the flow rates encountered the calculated loss in efficiency is 4 percent. Efficiencies less than 25 percent would change by less than one percentage point.

Perhaps more important than the loss of efficiency within the row are the temperature excursions which occur within the row due to flow variations. When the flow variations due to the nonuniform velocity distribution are present, the center collectors get the hottest in summer and are more likely to freeze in winter. Anti-freeze protection, when needed, is provided by flowing warm water through the collectors. The collectors with the lowest flow are most likely to freeze. The work in reference 4 showed that the installation of orifices in the inlet of each collector should significantly reduce the flow variation between collectors. To verify this experimentally, flow orifices have been installed in two of the rows for subsequent tests.

Table III gives a summary of the predicted and experimental results. This table contains: (1) the experimental efficiencies; (2) two predicted efficiencies for each collector design; (3) the calculated efficiencies assuming the collectors experienced the same degradation as those exposed to dry operation; and (4) the uncertainties in the efficiencies due to the stated uncertainties in the measured values. The first predicted efficiency was calculated using the same assumptions as the predicted efficiencies given in Table II. The second predicted efficiency was made using estimates of the capacitance effects, and also included the effect of flow variation between collectors in a field row. A separate prediction is given because of uncertainties in the appropriate capacitance for the different collector designs and because the flow variation effects were not directly measured. The authors believe that the capacitance values used in the analysis are conservative because when a transient analysis was made the experimental collector response was slower than predicted. The calculated efficiencies designated as "worse case degradation" began with the predicted efficiencies which included capacitance and flow effects. The "worse case degradation" efficiencies assumed that the collectors experienced the same degradation as those exposed to dry operation. This degradation was found from the results in reference 2. In the work of this reference the collectors were tested in an indoor facility. They were then exposed outdoors without any coolant for several days having high incident fluxes. The collectors were then retested. There was a decrease in efficiency due to dry operation for all collector designs. Table IV gives the parameters for the indoor test efficiency results for both the initial tests and the tests after dry operation had occurred.

It was expected that degradation, if any, in the field would not be as great as that caused by dry operation. This appears to be true for all the collector designs except the one glass - black chrome. Although most of the collectors in the SBTF field have not experienced dry operation, they briefly reached temperatures in excess of 120 C (250° F) during the operational shakedown and some degradation may have occurred.

Monthly data. - The data in Table II are for selected days within the time period covered. Data was recorded nearly 80 percent of the time, and uninterrupted data was recorded for an entire day approximately 70 percent of the time. Table V gives the diffuse insolation, the total horizontal insolation, the total insolation incident on the plane of the collectors, and the average inlet and ambient temperature for each full day of data.

In addition to the heat transferred to the fluid during the daytime, a second heat transfer was calculated for some collectors. This second heat transfer was the quantity of heat absorbed by the fluid from the time the heat transfer rate goes positive in the morning until it goes negative in the afternoon. This time period is shown on figure 6. This quantity of heat is designated as the no net loss heat transfer and is typically in excess of the daytime (sunrise to sunset) heat transfer. For example, in December the no net loss heat transfer exceeded the daytime heat transfer by 22 percent for the two glass - black chrome collectors. For all the days in December in which data was taken the no net loss heat transfer exceeded the daytime heat transfer by 39 percent. Figure 9 gives both the experimental and predicted efficiencies based on the no net loss heat transfer for the two glass - black chrome collectors. The predicted heat transfer was calculated on an hour by hour basis for a range on inlet temperatures using the December insolation and weather data. The calculation procedure is discussed in appendix A. For each hour of each day for which a negative heat transfer was calculated, a value of zero was used in summing up the heat transfer for the day. The experimental data point in figure 9 is derived from the total no net loss heat transfer for the month and is plotted at the average inlet temperature for which this heat was gained. The data in figure 9 illustrate the potential of the system when operated in a near optimum configuration. The

relative agreement between the predicted and experimental efficiencies in this figure is about the same as relative agreement between the predicted and experimental efficiencies based on all the daytime hours. Also illustrated in this figure is the effect of reducing the inlet temperature on the collector efficiency. If the required heat for the building could be delivered at a lower temperature, the efficiency of the system would be significantly improved.

CONCLUDING REMARKS

The initial results from the SBTF show the usefulness of the facility for conducting comparative collector tests. Data obtained over a 3½ month period show good consistency in the experimental efficiency for collectors of the same design. When collectors were compared that differed only in the emittance of the absorber plate, the advantage of a low emittance absorber coupled with a high absorptance was clearly shown in these tests.

The performance of collectors was compared with predicted efficiencies on a daily and monthly basis. Except for one collector design the difference between the predicted and experimental daytime efficiencies was generally less than five percentage points when averaged on a monthly basis. Estimates were made of the effect on the predicted collector efficiency due to the thermal capacitance of the collectors and the flow distribution within each row of collectors. The agreement between predicted and experimental performance was achieved over a wide range of weather, insolation, and operating conditions. The solar field yielded both performance data and helped satisfy the building's hot water requirements. Performing both tasks did not interfere with the acquisition of useful solar collector data.

APPENDIX A

PREDICTION OF COLLECTOR THERMAL PERFORMANCE

The prediction of the solar collector thermal performance is based on the work in references 5 and 6. The all day efficiency calculations are based on the design procedure given in reference 6. The procedure used to predict the efficiency of the collectors at the SBTF was to modify the equation giving the collectors "as received" thermal performance to account for the difference between the conditions at which the "as received" test was run and the conditions which prevailed during the SBTF testing. The prediction based on the "as received" data is first modified to account for the difference between the initial test flow rate and the SBTF experimental flow rate. Additional factors are introduced to account for the insolation not being normal to the surface of the collectors, for shading within individual collectors, for dust on the surface of the collectors, and for the difference between the SBTF experimental wind speed and the initial test wind speed.

Each collector design was subject to an initial test to determine its basic thermal performance. This work is described in reference 2. The basic efficiency data is given by the expression:

$$\eta = \frac{E_{or}H_{tp} - E_s(T_i - T_a)}{H_{tp}} \qquad (1)$$

This equation gives the collector efficiency at a mass flow rate, G_1, when the incident insolation, H_{tp}, is normal to the collector in terms of two parameters, E_{or} and E_s, which are determined experimentally. When the efficiency is plotted as a straight line function of $(T_i - T_a)/H_{tp}$, E_{or} gives the efficiency intercept and E_s gives the negative of the slope. Table IV lists the values of E_{or} and E_s from the experimental data in reference 2 and used in the analysis of this paper. Also included in this table are the values of E_{or} and E_s which were determined after the collectors had been exposed to dry operation.

The rate at which heat is absorbed by all of the collectors in a row is given by:

$$Q_e = F_R A_r\left[H_{tp}(\tau\alpha) - U_L(T_i - T_a)\right]$$
$$= \dot{m}_r C_p(T_{o,r} - T_i) \qquad (2)$$

From equation 7.74 of reference 5:

$$\frac{F_R}{F'} = \frac{\dot{m}_r C_p}{F' A_r U_L}\left[1 - \exp\left(\frac{-F' U_L A_r}{\dot{m}_r C_p}\right)\right] \qquad (3)$$

In this equation F' is the ratio of the heat transfer resistance from the absorber plate to the ambient air to the resistance from the fluid to the ambient air. The heat removal factor, F_R, is the ratio of the actual useful energy gain to the useful gain if the whole collector surface were at the fluid inlet temperature.

By definition:

$$G_r = \frac{\dot{m}_r}{A_r} \qquad (4)$$

When the mass flow rate, G_r, is equal to G_1

$$F_R\left[H_{tp}(\tau\alpha) - U_L(T_i - T_a)\right]$$
$$= E_{or}H_{tp} - E_s(T_i - T_a) \qquad (5)$$

Then:

$$E_s \frac{F'}{F_R} = U_L F' \qquad (6)$$

Equation (3) can be rewritten as:

$$\frac{F_{R,1}}{F'} = \frac{G_1 C_p}{E_s \frac{F'}{F_R}}\left[1 - \exp\left(\frac{-E_s F'}{G_1 C_p F_R}\right)\right] \qquad (7)$$

Solving for $F'/F_{R,1}$ results in:

$$\frac{F'}{F_{R,1}} = \frac{-\ln\left(1 - \frac{E_s}{G_1 C_p}\right)}{\frac{E_s}{G_1 C_p}} \qquad (8)$$

At the experimental mass flow rate, G_e, equation (3) becomes

$$\frac{F_{R,e}}{F'} = \frac{G_e C_p}{U_L F'}\left[1 - \exp\left(\frac{U_L F'}{G_e C_p}\right)\right] \qquad (9)$$

The assumption was made that U_L was not a function of the mass flow rate for small changes in the flow rate. In order to minimize the difference between the experimental flow rates and the initial test flow rate, the efficiency constants used in the analysis were those in Table IV for the lower flow rate of 24.4 kg/hr-m^2 (5 lb/hr-ft^2). The efficiency at the experimental mass flow rate and with the insolation normal to the collector is:

$$\eta = \frac{F_{R,e}}{F_{R,1}}\left[\frac{E_{or}H_{tp} - E_s(T_i - T_a)}{H_{tp}}\right] \qquad (10)$$

with:

$$\frac{F_{R,e}}{F'} = \frac{G_e C_p}{E_s \frac{F'}{F_{R,1}}}\left[1 - \exp\left(\frac{-E_s F'}{G_e C_p F_{R,1}}\right)\right] \qquad (11)$$

Except at solar noon the insolation is not normal to the collectors. To correct for this on a daily basis, reference 6 suggests that the transmittance-absorptance product ($\tau\alpha$), be multiplied by a factor, K_g, less than 1. For a two glass collector a value of 0.91 is recommended, and for a one glass collector a value of 0.93 is recommended. Reference 5 recommends the incident flux be reduced by 3 percent to account for shading within the collector and that the flux be further reduced by 2 percent when dust is likely to be present on the surface of the collectors. These values were used in the analysis. The resultant expression for the efficiency of the collectors on a daily basis is:

$$\eta = \frac{F_{R,e}}{F_{R,1}}\left[\frac{E_{or}K_g(0.97)(0.98)H_{tp} - E_s(T_i - T_a)}{H_{tp}}\right] \qquad (12)$$

In the initial tests the collectors were subjected to an equivalent wind speed of 11.3 km/hr (7 miles/hr), and were tilted to the same angle as the collectors installed in the SBTF. The predicted efficiency was modified to account for the effect of the experimental wind speed in the following manner. The loss coefficient, U_L, was calculated at both the initial test wind speed, yielding $U_{L,1}$, and at the experimental wind speed, yielding $U_{L,e}$. These calculations were made according to the procedure in reference 5 for flat plate collectors. The slope of the efficiency curve was then modified by the ratio of these two loss coefficients. The equation used to predict the efficiency of the collectors on a daily basis is:

$$\eta = \frac{F_{R,e}}{F_{R,1}}\left[\frac{E_{or}K_g(0.97)(0.98)H_{tp} - E_s U_{L,e}(T_i - T_a)/U_{L,1}}{H_{tp}}\right] \qquad (13)$$

The effects of the experimental wind speed were small. During December the average wind speed was 7.7 kph (4.8 mph). The predicted efficiencies at this wind speed were about one percentage point greater for two-glass collectors than those calculated using the indoor test wind speed of 11 kph (7 mph).

No net loss heat transfer prediction. - When the predicted no net loss heat transfer rate was calculated, it was done on an hour by hour basis. For each hour that a net heat loss was calculated for the collectors, zero heat gain was used in the analysis. Generally there was a net heat loss at the beginning and end of each day. The same procedure was used for the no net loss heat transfer prediction as for the daily heat transfer prediction except that the variable K_g became a function of the time of day. K_g was chosen as the ratio of the transmittance at time, t, during the day to the transmittance at solar noon.

$$K_g = \frac{\tau(t)}{\tau(\text{noon})} \qquad (14)$$

The transmittance, τ, was calculated according to the procedure given in reference 5 using an index of refraction of 1.526 for all collectors.

Insolation in collector plane. - The insolation in the plane of the collectors was found using measurements of the total insolation in the horizontal plane, and the diffuse insolation. Table V gives the total of these values for each day. A real time calculation is made at the SBTF to find the insolation on the collectors. The ratio of beam radiation on a tilted surface to that on a horizontal surface is calculated as a function of time using equation 3.6.2 from reference 5. The beam radiation was found from the difference between the total on the horizontal surface and the diffuse insolation rates. The total insolation on the collector plane was found by multiplying the beam radiation on the horizontal surface by the ratio of radiation on a tilted surface to that on a horizontal surface and adding in the diffuse insolation. Table V also contains the calculated values for the total insolation on the collector plane for each day.

For 5 weeks on either side of the winter solstice the outlet header cast a shadow on some collector rows. The first row, the Sunsource collectors, and the Libby-Owens-Ford collectors were not shadowed. Measurements indicated that during this time the length of the shadow was 7 percent of the length of the Chamberlain collectors near solar noon. To correct for the presence of the shadow the beam insolation was reduced by 7 percent in the all day analysis for those rows in the shadow. The average monthly efficiency was calculated without any shadow effect. The experimental data was adjusted to this condition by multiplying the no net

loss heat transfer rate by the predicted shadow effect. This effect was taken as the ratio of the monthly heat gained using the measured insolation to the monthly heat gained with the beam component of the insolation reduced by 7 percent when the shadow was present.

APPENDIX B

NOMENCLATURE

A - area, m^2 (ft^2)

C_p - specific heat, J/kg-C (Btu/lb-^oF)

E_{or} - constant giving the basic efficiency at the ordinate

E_s - the negative of the slope of the efficiency curve, W/m^2-C (Btu/hr-ft^2-^oF)

F_R - collector heat removal factor

F' - factor to account for resistance between absorber and fluid

G - mass flow rate per unit area, kg/m^2-hr (lb/ft^2-hr)

H - insolation, W/m^2 (Btu/ft^2-hr)

K_g - factor accounting for off-normal insolation

$\dot{m}$ - mass flow rate, kg/hr (lb/hr)

T - temperature, C (^oF)

t - time, hr

U_L - overall loss coefficient, W/m^2-C (Btu/hr-ft^2-^oF)

η - efficiency

τ - transmittance

$(\tau\alpha)$ - transmittance-absorbtance product

Subscripts:

a - ambient

c - center of collector row

d - diffuse

e - experimental

i - inlet

o - outlet

r - entire row

th - total on horizontal plane

tp - total on plane of collectors

1 - test condition for individual collector measurements

REFERENCES

(1) Knoll, R. H., et al., Initial Operation of a Solar Heating and Cooling System in a Full-Scale Solar Building Test Facility, NASA TM X-73519, 1976.

(2) Knoll, R. H. and Johnson, S. M., Baseline Performance of Solar Collectors for NASA Langley Solar Building Test Facility, NASA TM X-3505, 1977.

(3) Simon, F. F., Flat-Plate Solar-Collector Performance Evaluation with a Solar Simulator as a Basis for Collector Selection and Performance Prediction, NASA TM X-71793, 1975.

(4) Rohde, J. E. and Knoll, R. H., Analysis of a Solar Collector Water Flow Network, NASA TM X-3414, 1976.

(5) Duffie, J. A. and Beckman, W. A., Solar Energy Thermal Processes, John Wiley & Sons, Inc., New York, 1974.

(6) Klein, S. A., Beckman, W. A., and Duffie, J. A., A Design Procedure for Solar Heating Systems, Solar Energy, 18, 1976, pp. 113-127.

TABLE I. - DETAILS OF SBTF SOLAR COLLECTORS

Manufacturer	Glazing	Absorber surface and emittance[a] ( )	Absorber material and construction	Effective absorber area[b]		Nominal size of collector		Insulation	Number of rows in field	Area	
				m^2	ft^2	cm	in.			m^2	ft^2
Chamberlain	2 Glasses	Selective paint (0.6)	Steel plates spot and seam welded	2.03	21.9	243.8 by 91.4	96 by 36	5.08 cm (2 in.) Urethane foam	3	311	3348
Chamberlain	1 Glass	Black chrome (0.06)	Steel plates spot and seam welded	2.03	21.9	243.8 by 91.4	96 by 36	5.08 cm (2 in.) Urethane foam	2	207.4	2232
Chamberlain	2 Glasses	Black chrome (0.06)	Steel plates spot and seam welded	2.03	21.9	243.8 by 91.4	96 by 36	5.08 cm (2 in.) Urethane foam	3	311	3348
Sunsource	1 Glass	Black nickel (0.1)	Steel tubes mechanically bonded between two steel sheets	1.39	14.95	185.4 by 96.5	73 by 38	7.62 cm (3 in.) Fiberglass	1	58.3	628
General Electric	2 Lexan	Alcoa selective paint (0.38)	Aluminum roll bond	2.15	23.1	243.8 by 96.5	96 by 38	2.54 cm (1 in.) Fiberglass board plus 6.35 cm (2.5 in.) Urethane foam	1	109.4	1178
Libbey-Owens-Ford	2 Glasses	Black paint (0.97)	Aluminum roll bond	1.63	17.56	193.0 by 86.4	76 by 34	7.62 cm (3 in.) Fiberglass board	1	83.2	896
Martin-Marietta	2 Glasses	Optical black (0.94)	Aluminum roll bond	1.97	21.25	243.8 by 91.4	96 by 36	8.89 cm (3.5 in.) Vermiculite	1	100.7	1084

[a]Absorptances of all absorber surfaces was ~1.0.
[b]Net absorber plate area.

TABLE II. - COMPARISON OF PREDICTED AND EXPERIMENTAL DAYTIME EFFICIENCIES FROM OCTOBER 1976 TO JANUARY 1977

		Collector design																					
		Chamberlain														Sunsource		Martin		L.O.F.		G.E.	
		Number of covers																					
		2		2		2		1		1		2		2		2		1		2		2		2	
		Plate emittance																					
		0.6		0.6		0.6		0.06		0.06		0.06		0.06		0.06		0.1		0.94		0.97		0.38	
		Row																					
		1		2		7		8		9		10		11		12		3		4		5		6	
		Collector efficiency, %																					
Month	Day	Exp.	Pre.	Exp.	Pre.	Exp.	Pre.	Exp.	Pre.	Exp.	Pre.	Exp.	Pre.	Exp.	Pre.	Exp.	Pre.	Exp.	Pre.	Exp.	Pre.	Exp.	Pre.	Exp.	Pre.
0	2	10.8	6.1	13.4	6.0	18.5	6.7	22.7	24.2	19.7	24.8	22.3	15.7	----	----	----	----	11.5	-0.1	---	----	----	----	9.0	9.9
	5	15.3	12.4	15.8	14.9	17.2	15.1	23.9	31.8	20.5	31.9	22.5	23.7	----	----	----	----	11.9	7.7	---	----	2.0	3.7	11.0	19.4
	7	16.5	10.4	13.0	11.5	14.8	11.4	22.8	29.5	20.0	29.5	21.8	20.8	----	----	----	----	14.0	4.6	---	----	-.4	8.9	11.6	15.1
	10	20.1	24.9	22.1	25.8	30.2	26.7	38.6	42.6	36.4	41.7	36.0	33.2	20.3	33.0	----	----	18.3	21.0	---	----	----	----	30.9	27.9
	11	22.1	16.7	12.4	14.2	20.9	17.4	25.4	32.6	21.8	33.4	24.1	24.6	----	----	----	----	11.5	9.7	---	----	----	----	21.9	21.8
	12	10.5	10.8	7.9	13.6	11.0	14.1	18.2	30.1	15.1	30.6	17.0	22.6	----	----	----	----	6.4	6.2	---	----	----	----	7.7	18.3
	13	24.6	22.8	29.4	27.1	30.3	27.2	38.8	43.3	35.8	43.5	36.0	33.9	----	----	----	----	17.9	21.1	---	----	20.0	17.9	29.8	32.5
	14	19.2	18.1	22.9	20.4	22.8	20.3	31.2	36.8	28.4	36.9	29.7	28.5	23.7	27.3	----	----	15.4	13.4	---	----	11.3	9.7	18.5	24.9
	15	23.2	20.5	28.1	22.8	24.8	22.6	34.8	39.5	31.6	39.7	32.4	30.2	31.4	29.7	----	----	19.2	17.4	---	----	14.2	12.7	22.5	27.3
	16	----	----	18.7	18.3	16.9	18.6	26.6	34.4	23.5	34.9	24.9	26.4	----	----	----	----	9.8	10.8	---	----	5.8	7.9	14.0	23.0
	18	9.2	12.5	5.8	13.7	7.3	13.7	15.7	30.3	13.5	30.5	15.5	22.6	----	----	----	----	4.2	5.5	---	----	-1.7	2.1	8.9	17.8
	21	22.3	23.1	21.7	25.3	24.2	25.7	31.6	41.7	30.1	41.9	30.6	32.8	----	----	----	----	18.5	19.9	---	----	14.4	15.9	25.2	30.8
	22	13.0	17.5	12.3	18.0	11.2	18.0	20.1	34.2	18.3	34.3	20.1	26.6	----	----	----	----	8.6	11.0	---	----	-1.4	7.0	8.8	22.5
	23	----	----	----	----	14.6	15.0	11.9	31.8	14.3	29.4	----	----	----	----	----	----	----	----	---	----	15.0	6.9	----	----
	29	26.1	12.1	24.3	13.0	23.4	12.9	32.9	30.6	29.5	30.7	31.1	22.2	29.9	21.6	----	----	21.5	6.2	---	----	11.8	1.2	19.7	16.6
Average		17.9	16.0	17.7	17.5	19.2	17.7	26.4	34.2	23.9	34.3	26.0	26.0	26.3	27.9	----	----	13.5	11.0	---	----	8.3	11.0	17.1	22.0
Difference		1.9		0.2		1.5		-7.8		-10.4		0.0		-1.6		----		2.5		----		-2.7		-4.9	
11	7	20.2	19.7	16.1	19.9	18.5	20.0	33.1	46.6	31.5	46.6	25.2	27.7	----	----	----	----	19.1	14.8	---	----	10.6	9.7	14.9	24.6
	11	24.5	20.3	11.1	20.5	15.9	20.1	27.0	35.0	24.2	35.8	22.6	28.4	20.3	28.3	22.0	28.4	20.3	16.2	---	----	----	----	----	----
	13	20.8	25.3	13.7	27.1	15.1	27.1	23.7	37.4	21.2	37.4	24.1	33.6	22.3	32.6	20.7	32.7	18.3	24.3	---	----	----	----	----	----
	16	22.4	17.1	17.4	17.2	16.1	17.2	23.2	41.5	23.3	42.5	22.7	26.3	21.8	25.9	20.2	26.2	17.5	11.9	---	----	----	----	----	----
	23	9.0	10.3	4.3	4.6	9.2	6.8	11.9	21.2	14.3	22.3	18.0	17.2	13.8	17.5	15.2	17.2	8.4	1.1	2.3	-0.4	-.6	-1.8	5.3	5.6
	25	14.8	14.5	----	----	9.1	13.5	----	----	16.1	30.3	17.3	22.1	19.4	23.0	17.4	22.4	9.8	8.7	---	----	----	----	9.3	16.2
	27	19.6	11.6	9.4	7.7	19.2	8.8	----	----	14.5	21.6	20.0	18.2	28.7	18.9	25.5	18.5	16.9	3.7	---	----	----	----	----	----
Average		18.8	17.0	12.0	16.2	15.2	16.2	23.8	36.5	20.7	33.8	22.1	24.8	21.1	24.4	20.2	24.2	15.8	11.5	2.3	-0.4	5.0	4.0	9.8	15.5
Difference		1.8		-4.2		-1.0		-12.5		-13.1		-2.7		-3.3		-4.0		4.3		2.7		1.0		-5.7	
12	3	9.6	10.0	1.2	6.4	6.0	6.8	11.8	23.2	10.7	23.2	13.5	17.1	----	----	14.1	17.6	5.7	0.9	---	----	----	----	4.9	10.0
	4	12.2	19.0	----	----	8.4	14.3	9.0	30.0	16.6	33.5	18.4	24.2	----	----	----	----	9.5	14.6	---	----	----	----	8.7	18.7
	5	15.0	20.8	8.0	15.6	----	----	----	----	17.7	32.1	18.9	24.7	----	----	----	----	8.9	14.0	---	----	----	----	10.7	20.0
	14	17.2	17.1	10.2	13.4	12.2	13.6	21.7	29.9	20.4	30.0	20.7	22.3	----	----	----	----	11.2	10.4	---	----	----	----	11.9	17.9
	17	----	----	----	----	5.0	17.4	13.5	32.7	10.1	32.9	13.6	25.9	----	----	----	----	3.1	13.7	---	----	----	----	----	----
	18	21.2	25.7	20.4	22.2	23.4	22.1	30.6	37.2	29.7	37.4	29.1	29.5	----	----	----	----	22.1	20.6	---	----	----	----	----	----
	22	----	----	----	----	-3.2	4.6	9.0	30.0	2.8	23.0	6.7	15.4	7.8	15.5	11.7	15.0	-.7	-.8	---	----	----	----	----	----
	23	3.0	7.8	1.0	4.2	3.0	4.1	10.2	20.6	8.8	20.7	12.2	15.0	12.8	15.2	11.1	15.3	3.0	-2.0	---	----	----	----	----	----
	24	21.2	18.2	12.5	15.3	14.4	14.8	21.1	31.0	20.0	30.1	21.8	23.9	22.6	24.2	21.6	24.3	15.1	11.2	---	----	----	----	----	----
	27	9.7	16.0	3.7	12.4	8.4	12.2	15.1	27.6	14.4	27.8	16.2	22.0	17.2	22.3	15.5	22.3	5.5	7.4	---	----	----	---	----	----
Average		13.6	16.8	8.1	12.8	8.6	12.2	15.8	29.1	15.1	29.1	17.1	22.0	15.1	19.3	14.8	18.9	8.3	9.0	---	----	----	---	9.1	16.7
Difference		-3.2		-4.7		-3.6		-13.3		-14.0		-4.9		-4.2		-4.1		-0.7		----		----		-7.6	
1	11	6.5	13.9	----	----	5.3	10.3	12.3	26.2	10.4	26.2	13.5	20.8	13.9	20.8	11.2	20.9	----	----	---	----	-5.6	1.5	4.6	14.2
	12	8.1	16.3	5.9	12.9	8.9	12.5	15.6	28.7	14.1	28.8	15.9	22.0	16.9	22.3	15.1	22.4	----	----	---	----	-1.2	4.8	7.9	16.8
	15	28.9	20.3	18.5	16.7	17.4	16.6	23.5	32.9	21.7	33.0	22.9	24.5	25.6	25.4	22.7	24.6	----	----	---	----	11.6	9.8	17.6	21.2
Average		14.5	16.8	12.2	14.8	10.5	13.1	17.1	29.3	15.4	29.3	17.4	22.4	18.8	22.8	16.3	22.6	----	----	---	----	4.8	5.4	10.0	17.4
Difference		-2.3		-2.6		-2.6		-12.2		-13.9		-5.0		-4.0		-5.3		----		----		-0.6		-7.4	

TABLE III. - MONTHLY AVERAGE OF EFFICIENCIES FOR SELECTED DAYS FOR VARIOUS COLLECTOR DESIGNS

Collector design	Efficiency, %				Efficiency uncertainty due to stated measurement uncertainty, %
	Experimental	Predicted		Calculated assuming worst case degradation occurred[a]	
		Based on all day analysis from appendix A	Including estimates of heat capacity and flow effects		
October 1976					
Chamberlain 2 glass-black chrome	26.1	26.4	21.9	16.8	±1.5
Chamberlain 1 glass-black chrome	25.1	34.2	30.4	27.2	±1.7
Chamberlain 2 glass-Sel. pt.	18.3	17.1	13.5	6.6	±1.8
Sunsource 1 glass	13.5	11.0	6.6	3.3	±1.6
General Electric 2 Lexan	17.1	22.0	19.4	13.5	±2.4
Libby-Owens-Ford 2 glass	8.3	11.0	8.8	3.9	±1.7
November 1976					
Chamberlain 2 glass-black chrome	21.2	24.5	18.2	13.2	±1.3
Chamberlain 1 glass-black chrome	22.0	34.8	29.7	26.6	±1.5
Chamberlain 2 glass-Sel. pt.	15.5	16.5	11.4	4.6	±1.6
Sunsource 1 glass	15.8	11.5	5.0	1.5	±1.9
General Electric 2 Lexan	9.8	15.5	12.2	6.9	±1.4
Libby-Owens-Ford 2 glass	5.0	4.0	1.1	-3.7	±1.5
December 1976					
Chamberlain 2 glass-black chrome	16.1	20.6	17.9	12.7	±1.3
Chamberlain 1 glass-black chrome	15.4	29.1	26.6	23.5	±1.3
Chamberlain 2 glass-Sel. pt.	10.1	13.9	11.8	4.8	±1.7
Sunsource 1 glass	8.3	9.0	6.5	3.4	±1.7
General Electric 2 Lexan	9.1	16.7	15.1	10.1	±1.2

[a]Using data from ref. 2.

TABLE IV. - EFFICIENCY PARAMETERS USED IN THE ANALYSIS

Collector Manufacturer/Design	Initial tests				After dry operation	
	Mass flow rate per unit area, G_1, kg/m^2-hr					
	24.4		48.8		48.8	
	Efficiency constants					
	E_{or}	E_s, W/m^2-C	E_{or}	E_s, W/m^2-C	E_{or}	E_s, W/m^2-C
Chamberlain 2 glass, Sel. pt.	0.620	43.9	0.685	45.2	0.635	48.6
Chamberlain 1 glass, black chrome	0.770	41.9	0.830	40.0	0.814	42.2
Chamberlain 2 glass, black chrome	0.655	36.4	0.713	33.3	0.693	38.1
Sunsource 1 glass	0.660	57.9	0.747	63.8	0.647	58.0
General Electric 2 Lexan	0.700	47.2	0.711	43.8	0.620	41.4
Libby-Owens-Ford 2 glass	0.580	52.9	0.637	54.8	0.614	58.6
Martin-Marietta 2 glass	0.615	51.3	0.660	52.8	0.660	54.2

TABLE V. - DAILY INSOLATION (DIFFUSE, TOTAL HORIZONTAL, AND TOTAL IN C[illegible]OR PLANE) AND AVERAGE AMBIENT AND INLET TEMPERATURES FOR THE TEST PERIOD OF OCTOBER 1976 THROUGH MID-JANUARY 1977

Day	Month																			
	October					November					December					January				
	H_d, kJ/m²-day	H_{th}, kJ/m²-day	H_{tp}, kJ/m²-day	T_a, C	T_i, C	H_d, kJ/m²-day	H_{th}, kJ/m²-day	H_{tp}, kJ/m²-day	T_a, C	T_i, C	H_d, kJ/m²-day	H_{th}, kJ/m²-day	H_{tp}, kJ/m²-day	T_a, C	T_i, C	H_d, kJ/m²-day	H_{th}, kJ/m²-day	H_{tp}, kJ/m²-day	T_a, C	T_i, C
1	(a)	(a)	(a)	(a)	(a)	(b)	(b)	(b)	(b)	(b)	(a)	(a)	(a)	(a)	(a)	(b)	(b)	(b)	(b)	(b)
2	5910	8 710	9 700	17	49	↓	↓	↓	↓	↓	2950	10 800	18 450	9	83	↓	↓	↓	↓	↓
3	3360	3 790	3 950	14	34	↓	↓	↓	↓	↓	3070	10 480	17 440	2	61	↓	↓	↓	↓	↓
4	3430	3 900	4 080	16	33	↓	↓	↓	↓	↓	1240	10 520	19 600	7	64	↓	↓	↓	↓	↓
5	6270	11 590	13 620	17	53	(a)	(a)	(a)	(a)	(a)	1340	9 650	17 170	7	53	↓	↓	↓	↓	↓
6	(a)	(a)	(a)	(a)	(a)	(b)	(b)	(b)	(b)	(b)	3190	6 630	10 050	9	61	(b)	(b)	(b)	(b)	(b)
7	5970	13 780	16 900	19	69	2060	12 130	19 230	13	62	940	940	940	12	48	5010	7 862	10 240	6	54
8	6050	10 500	12 370	20	59	4940	8 980	11 920	7	44	1050	1 050	1 050	3	53	1160	10 470	18 780	2	74
9	5300	6 020	8 420	18	43	3170	11 480	17 800	7	53	(a)	(a)	(a)	(a)	(a)	2640	4 460	6 330	4	54
10	4400	17 310	22 910	13	57	(a)	(a)	(a)	(a)	(a)	3100	8 670	14 300	8	64	3150	5 250	7 020	9	56
11	5930	11 660	14 260	13	50	1730	11 610	18 920	12	62	3760	3 760	3 760	11	26	1300	11 040	19 780	1	62
12	5860	11 900	14 640	13	54	720	720	720	6	34	(b)	(b)	(b)	(b)	(b)	1360	10 900	19 340	3	61
13	4600	16 190	21 600	15	56	1600	12 370	20 670	7	49	(b)	(b)	(b)	(b)	(b)	1000	1 000	1 000	3	49
14	4010	15 740	21 190	16	66	4770	8 110	10 960	7	47	1020	9 860	18 410	6	61	(b)	(b)	(b)	(b)	(b)
15	2290	15 060	21 240	17	66	680	680	680	6	41	2120	2 120	2 120	7	51	3210	9 810	15 400	5	49
16	5390	13 890	17 950	16	61	2000	11 290	18 570	8	62	4180	4 180	4 180	9	53	3330	6 930	10 250	4	55
17	510	510	510	11	26	(a)	(a)	(a)	(a)	(a)	2520	9 180	15 760	8	49	1670	11 720	20 180	5	48
18	4510	13 100	17 730	10	61	(b)	(b)	(b)	(b)	(b)	1330	9 580	17 480	7	46					
19	6580	11 950	14 880	12	61	(b)	(b)	(b)	(b)	(b)	4080	6 830	9 530	10	59	Test terminated				
20	1360	1 500	1 570	16	39	(b)	(b)	(b)	(b)	(b)	2750	4 110	5 710	12	57					
21	2650	15 310	22 160	12	58	(b)	(b)	(b)	(b)	(b)	2860	8 380	14 010	3	54					
22	2840	16 010	23 160	12	71	6110	9 410	12 130	7	68	1480	9 930	18 080	1	70					
23	2860	15 300	22 070	13	73	3260	11 070	17 950	7	66	1942	9 230	15 470	7	68					
24	3370	4 020	4 400	12	23	(b)	(b)	(b)	(b)	(b)	1170	9 960	18 450	2	54					
25	4080	5 300	5 990	15	34	3860	8 930	13 630	11	51	3740	7 280	10 970	7	54					
26	(b)	(b)	(b)	(b)	(b)	(b)	(b)	(b)	(b)	(b)	2310	7 840	12 930	8	53					
27	(b)	(b)	(b)	(b)	(b)	3920	8 100	11 780	16	54	1060	10 040	18 600	3	58					
28	(b)	(b)	(b)	(b)	(b)	1150	1 180	1 230	14	21	3700	7 510	10 610	11	51					
29	2810	13 250	19 360	11	67	440	440	440	7	24	1820	2 170	2 570	4	29					
30	(b)	(b)	(b)	(b)	(b)	(a)	(a)	(a)	(a)	(a)	(a)	(a)	(a)	(a)	(a)					
31	(b)	(b)	(b)	(b)	(b)	--	------	------	---	----	(b)	(b)	(b)	(b)	(b)					

[a]Data recorded only for part of day.
[b]No data recorded during day.

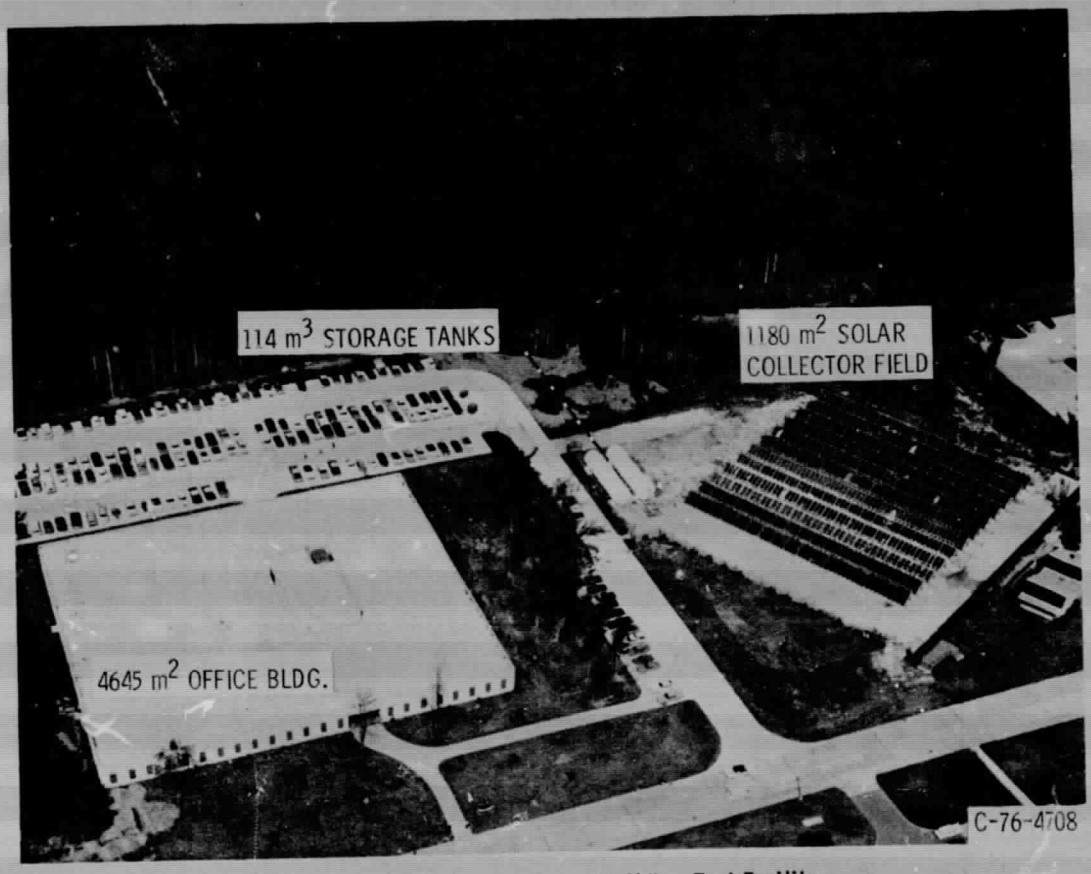

Figure 1. - The Langley Solar Building Test Facility.

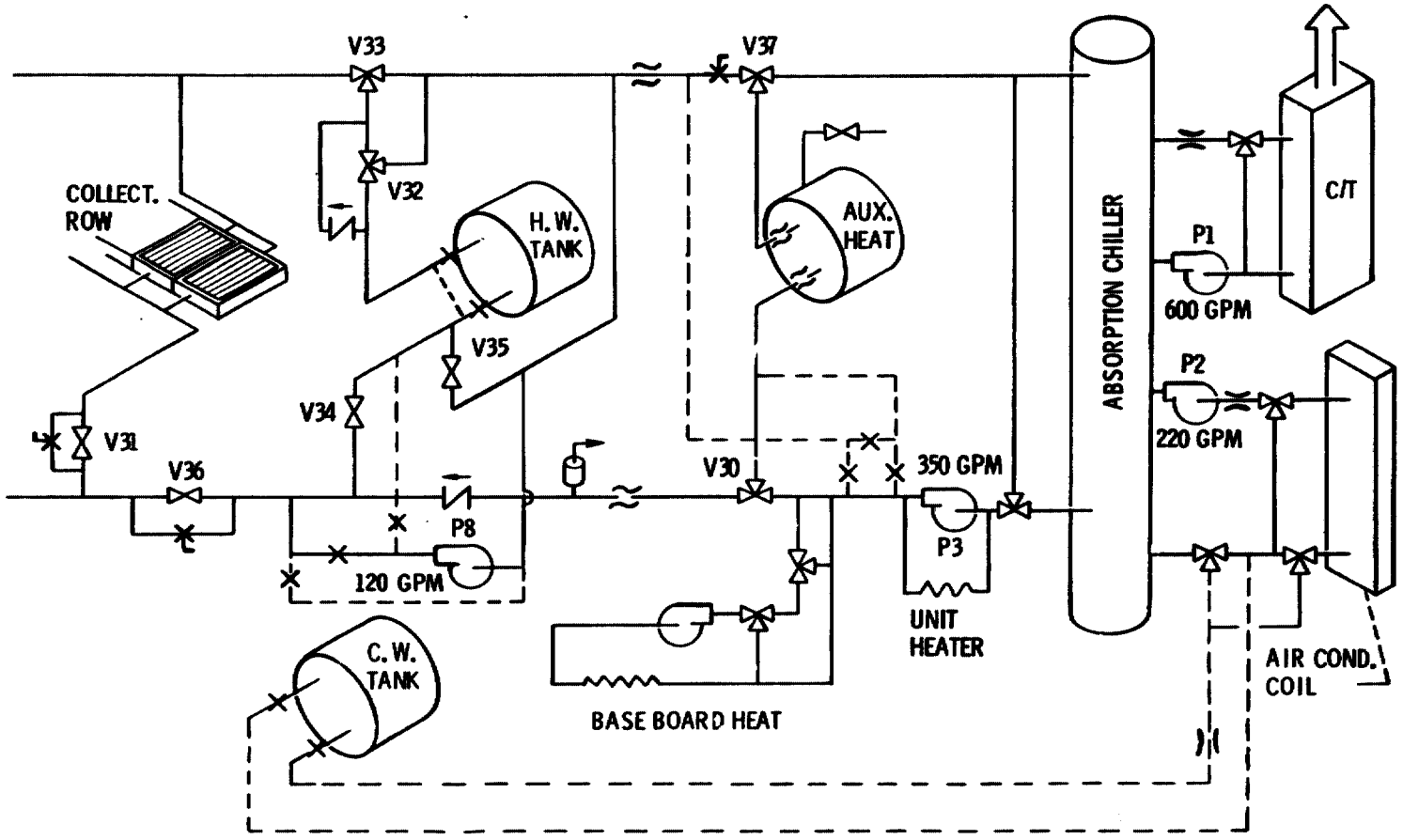

Figure 2. - Flow schematic for SBTF.

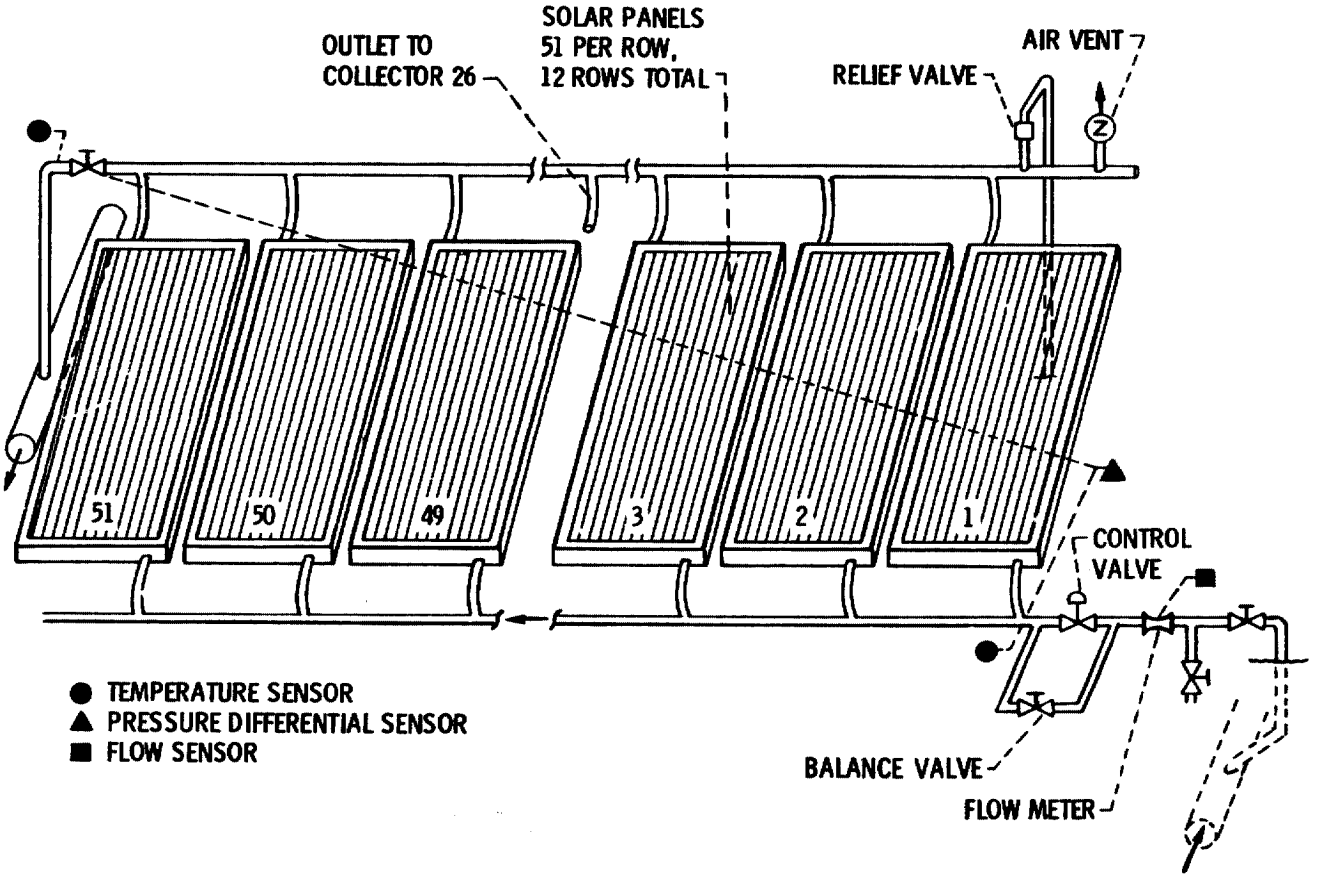

Figure 3. - Instrumentation for collector row 4 (typical for all rows).

↑ NORTH

COMPANY	GLAZING	COATING	ROW
CHAMBERLAIN	2 GLASS	BLACK CHROME	12
CHAMBERLAIN	2 GLASS	BLACK CHROME	11
CHAMBERLAIN	2 GLASS	BLACK CHROME	10
CHAMBERLAIN	1 GLASS	BLACK CHROME	9
CHAMBERLAIN	1 GLASS	BLACK CHROME	8
CHAMBERLAIN	2 GLASS	BLACK PAINT	7
GENERAL ELECTRIC	2 LEXAN	ALCOA SELECT.	6
LIBBEY-OWENS-FORD	2 GLASS	BLACK PAINT	5
MARTIN MARIETTA	2 GLASS	BLACK ANODIZED AL.	4
SUN SOURCE	1 GLASS	TABOR (BLK. Ni)	3
CHAMBERLAIN	2 GLASS	BLACK PAINT	2
CHAMBERLAIN	2 GLASS	BLACK PAINT	1

NOTE: ALL ROWS CONTAIN 51 COLLECTORS EACH EXCEPT ROW 3 WHICH CONTAINS 42 COLLECTORS.

Figure 4. - Initial collector field layout.

Figure 5. - Most of collector designs in SBTF field.

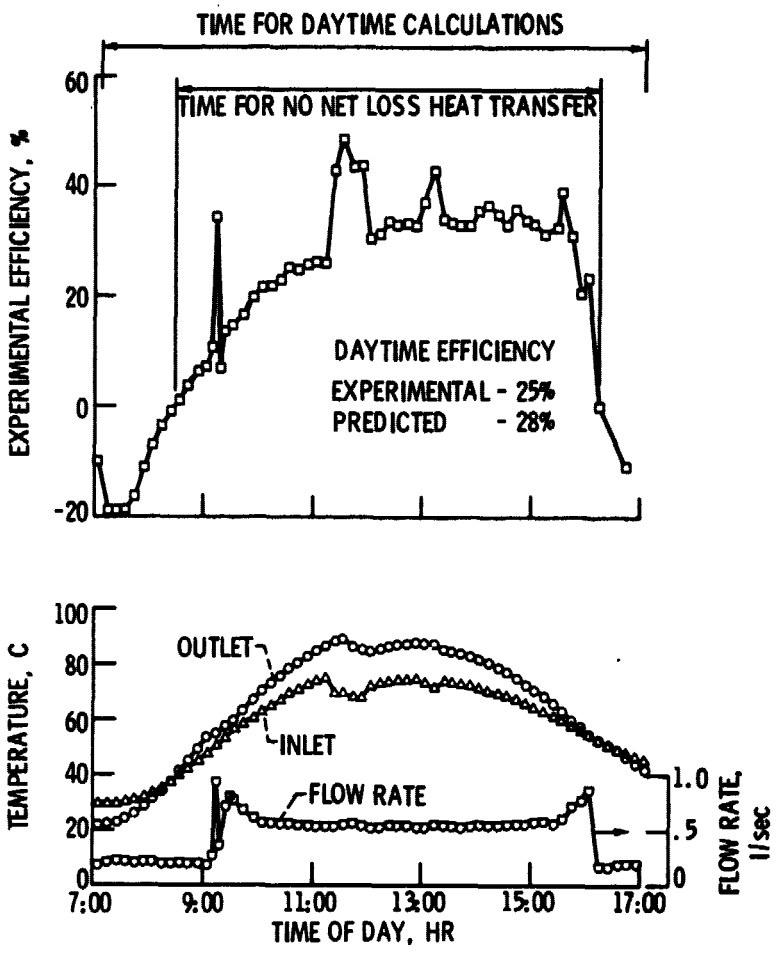

Figure 6. - Typical daytime measurements and predicted efficiency for row 10 on 11/7/76; 2 glass black chrome collectors.

COLLECTOR TYPE											
CHAMBERLAIN								SUNSOURCE	MARTIN	L.O.F.	G.E.
NUMBER OF COVERS											
2	2	2	1	1	2	2	2	1	2	2	2
PLATE EMITTANCE											
0.6	0.6	0.6	0.06	0.06	0.06	0.06	0.06	0.1	0.94	0.97	0.38
ROW											
1	2	7	8	9	10	11	12	3	4	5	6

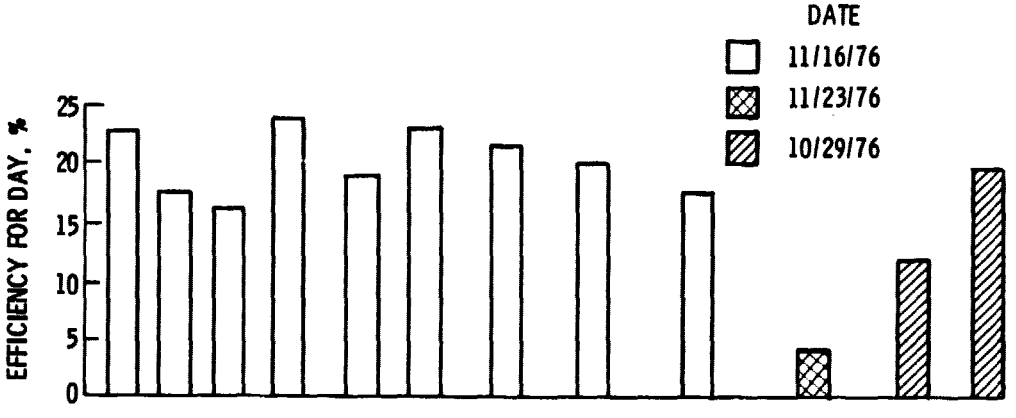

Figure 7. - Selected daily efficiency comparisons of collector designs in field.

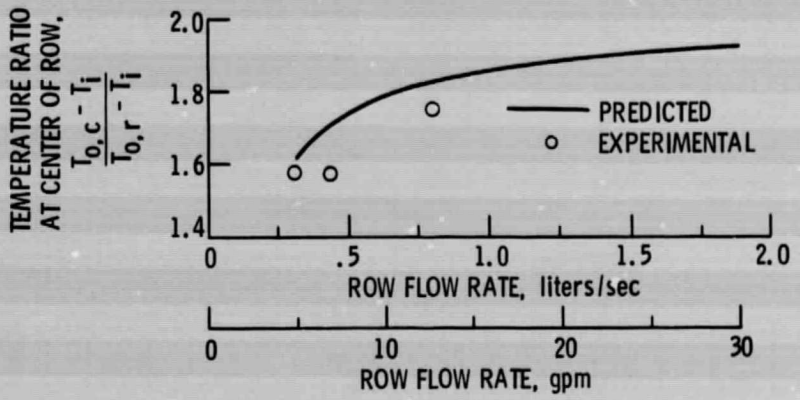

Figure 8. - Ratio of temperature difference between outlet and inlet at center of row and temperature difference for the entire row; 2 glass black chrome collector.

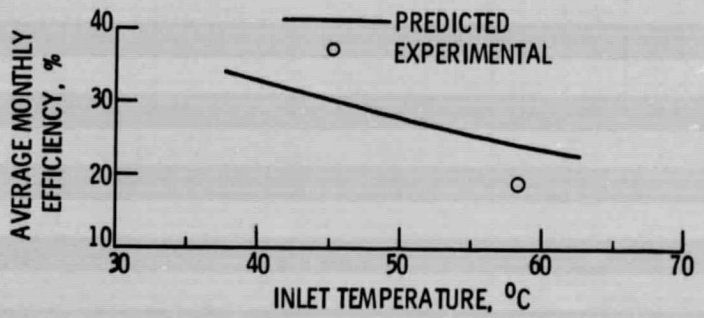

Figure 9. - Effect of row inlet temperature on the no net loss collector efficiency, 2 glass-black chrome collector, Dec. insolation and weather data.